Retreat of the Laurentide ice sheet tracked by the isotopic composition of Pb in western North Atlantic seawater during termination 1

Marcus Gutjahr[1, 2], Martin Frank[1,3], Alex N. Halliday[4] & Lloyd D. Keigwin[5]

[1] *Institute for Isotope Geochemistry and Mineral Resources, Department of Earth Sciences, ETH Zürich, 8092 Zürich, Switzerland*

[2] *Bristol Isotope Group, Department of Earth Sciences, University of Bristol, Wills Memorial Building, Bristol BS8 1RJ, UK*

[3] *IFM-GEOMAR, Leibniz Institute of Marine Sciences at the University of Kiel, 24148 Kiel, Germany*

[4] *Department of Earth Sciences, University of Oxford, Parks Road, Oxford OX1 3PR, UK*

[5] *Woods Hole Oceanographic Institution, Woods Hole, MA 02543, U.S.A.*

Word count : abstract 315 ; body text 4,765 ; 60 references ; 8 figures ; 1 table; 1 supplementary table.

Abstract

During the Last Glacial Maximum much of North America was covered by the Laurentide ice sheet. Its melting during termination 1 led to systematic changes in proglacial lake formation, continental runoff, and possibly North Atlantic Meridional Overturning Circulation. The accompanying change in chemical weathering rates in the interior of North America throughout the deglaciation resulted in a pronounced change in seawater Pb isotope composition in the western North Atlantic Ocean. Here we present the first high-resolution records of seawater Pb isotope variations of North Atlantic Deep Water extracted from authigenic Fe-Mn oxyhydroxides in three sediment cores (51GGC, 1790 m depth; 31GGC, 3410 m depth; 12JPC, 4250 m depth) from the Blake Ridge off Florida. These data reveal a striking excursion from relatively unradiogenic $^{206}Pb/^{204}Pb$ as low as 18.93 towards highly radiogenic Pb isotope compositions that was initiated during the Bølling-Allerød interstadial and was most pronounced in both intermediate and deep waters during and after the Younger Dryas ($^{206}Pb/^{204}Pb$ as high as 19.38 at 8.8 ka in 4250 m). This pattern is interpreted to be a direct function of increased inflow of continent-derived radiogenic Pb into the western North Atlantic, supplied through chemical weathering of North American rocks that had been eroded and freshly exposed during the preceding glacial cycle. These sediment-derived data are complemented by new laser ablation Pb isotope data from a ferromanganese crust from the Blake Plateau at 850 m water depth, which show only small glacial-interglacial Pb isotope variations of the Florida Current ($^{206}Pb/^{204}Pb$ between 19.07 and 19.16). The lack of change in the Blake Plateau record at the same time as the radiogenic excursion in the deeper sediments supports a northern origin of the pulse of radiogenic Pb. After the Younger Dryas, the deep western North Atlantic has experienced a persistent highly radiogenic Pb supply

that was most pronounced during the first half of the Holocene and still lasts until today.

1. Introduction

The Pleistocene (1.8 Ma to 10 ka BP) was an extreme climatic period during which the geomorphology of the mid and high latitudes in both hemispheres was strongly modulated by a sequence of glacial advances and interglacial retreats of continental ice sheets, resulting in efficient continental denudation. During most of the Pleistocene, large areas of North America were covered by the Laurentide ice sheet (e.g., Joyce et al., 1993; Dyke et al., 2002; Clark et al., 2006). On average an estimated 120 m of rock was physically eroded by the ice sheets since the onset of the major glaciations (Bell and Laine, 1985). In contrast, chemical weathering rates were significantly reduced in North America due to persistent ice coverage during the last glacial period (Marshall and Clark, 2002). At the same time non-glaciated North American regions experienced colder climatic conditions, which are also expected to have resulted in reduced chemical weathering rates (Tranter et al., 2002; Millot et al., 2003; White et al., 2003; West et al., 2005; Gislason et al., 2009).

The major climatic transitions at glacial terminations created significant changes in the chemical weathering rates and cation runoff flux (Anderson et al., 2000; Foster and Vance, 2006; Gislason et al., 2009; Vance et al., 2009). Glacially eroded rock substrate was increasingly exposed to the atmosphere in a warming climate (Marshall and Clarke, 1999). The resulting strongly enhanced cation runoff flux from the Laurentide region is expected to be recorded in adjacent ocean basins such as the Gulf

of Mexico or the western North Atlantic, which received an integrated weathering signal of deglacial warming in North America.

The evolution of the dissolved Pb flux transferred from the continents to the oceans and the related changes in the Pb isotope composition of seawater are promising indicators of such large scale weathering trends. In seawater, Pb is highly particle reactive with a residence time on the order of 20 to 30 years in the Atlantic (Henderson and Maier-Reimer, 2002) and 200-400 years in the Pacific (Craig et al., 1973; Schaule and Patterson, 1981). This is significantly shorter than the timescales of Atlantic and global overturning circulation. Because of its short residence time in seawater Pb is not advected over long distances or between ocean basins and merely reflects a local input signal although it has been used to reconstruct short distance water mass mixing (Abouchami and Goldstein, 1995; von Blanckenburg et al., 1996). The seawater Pb isotope composition recorded in ferromanganese crusts and marine sediments has been used to infer long-term changes in deep water circulation and continental inputs (Christensen et al., 1997; Abouchami et al., 1999; Frank et al., 1999a; Reynolds et al., 1999; Frank et al., 2002; Haley et al., 2008), as well as reorganisations of oceanic gateways (Burton et al., 1997; Frank et al., 1999b).

Lead is released incongruently during early chemical weathering on the continents and it has more recently been suggested that oceanic Pb isotopic records reflect this process. The specific incongruent chemical weathering behaviour that is responsible for a weathering signal in the Pb isotope system has been the focus of a number of studies in the past decade (Harlavan et al., 1998; Harlavan and Erel, 2002; Erel et al., 2004; Foster and Vance, 2006). Those studies focusing on Pb-specific chemical

weathering trends noted systematic differences in the released solute Pb isotope signal in soil chronosequences. In particular, in newly-produced or freshly exposed soils, accessory mineral phases rich in uranium (U) and thorium (Th) preferentially released highly radiogenic Pb during incipient and early chemical weathering, a solute signal that is significantly more radiogenic than the bulk rock Pb isotope composition. The magnitude of this incongruent chemical weathering pattern will depend on the abundance of U- and Th-rich mineral phases and the prevailing continental climatic conditions. Major shifts towards more radiogenic compositions found in NW Atlantic ferromanganese crust over the past 3 Myr (Burton et al., 1997; O'Nions et al., 1998; Reynolds et al., 1999) were explained in terms of incongruent weathering processes in Greenland and Canada (von Blanckenburg and Nägler, 2001). These authors also provided experimental evidence for the incongruent release of highly radiogenic Pb from a labile fraction in continental detritus eroding into the Labrador Sea.

In contrast to the previous coarse resolution studies that had a time resolution on the order of several 10s to 100 kyr, the first higher resolution record of the Pb isotope evolution over the last 500 kyr was obtained by laser ablation at a temporal resolution of around 10 kyr (Foster and Vance, 2006). Glacial-interglacial variations in the Pb isotopic composition of western North Atlantic intermediate depth water were resolved that tracked the benthic oxygen isotope record (Imbrie et al., 1984). From these records two- to three-fold glacial reductions in chemical weathering rates in the glaciated interior of North America have been deduced. However, despite the significantly higher resolution achieved by these authors compared with previous work, potential millennial and sub-millennial Pb isotope variations were still not resolvable.

Hence although substantial progress has been made in deciphering Pleistocene North Atlantic marine Pb isotope records over the past decade, sub-millennial changes of the past seawater Pb isotope compositions have as yet not been resolvable due to the lack of suitable paleoceanographic archives. Given the rate at which Northern Hemisphere climate changed during deglaciations (e.g., Steffensen et al., 2008) and the short duration of paleoceanographic perturbations such as the deposition of ice rafted debris during Heinrich events over the last glacial cycle (Hemming, 2004), it is essential to use paleoceanographic archives offering sub-millennial resolution. Here we present the first high-resolution records of Pb isotopic variations in North Atlantic Deep Water (NADW) at sub-millennial resolution extracted from authigenic Fe-Mn oxyhydroxides in marine sediments from the Blake Ridge in the western North Atlantic spanning the transition from the Last Glacial Maximum (LGM) to the Holocene (Fig. 1). We used a gentle reductive extraction method to isolate the authigenic seawater-derived Pb fraction from Fe-Mn oxyhydroxides in marine sediments (Gutjahr et al., 2007), allowing the investigation of the timing of events at glacial-interglacial transitions at an unprecedented temporal resolution. The new data are put in context of published ferromanganese crust records of Upper NADW (Reynolds et al., 1999; Foster and Vance, 2006) and a new laser ablation Pb isotope record obtained from a ferromanganese crust from the Blake Plateau tracing the glacial-interglacial Pb isotope evolution of the Florida Current over the past 200 kyr.

2. Material and Methods

Three cores retrieved during the KNR140 cruise along the Blake Ridge in the western North Atlantic spanning the interval from the LGM to the present day were selected

for Pb isotope analyses. Core 51GGC from 1790 m depth, 31GGC from 3410 m depth and 12JPC from 4250 m depth were sampled to monitor the seawater Pb isotope evolution in the intermediate and deep western North Atlantic (Fig. 1). At present-day the three core sites are situated within NADW. The Nd isotope composition of past seawater extracted from the Fe-Mn oxyhydroxides of the same samples were published earlier (Gutjahr et al., 2008) and suggested that the two lower core sites were bathed in a different water mass than NADW during the deglaciation until the Younger Dryas, which was likely advected from the South (Southern Source Water) (e.g., Boyle and Keigwin, 1987; Curry and Oppo, 2005; Lynch-Stieglitz et al., 2007).

The seawater signal was extracted from the marine sediments employing a sequential leaching technique described in Gutjahr et al. (2007). Dried bulk sediments were decarbonated with a Na acetate buffer and the weakly adsorbed fraction was removed using 1M $MgCl_2$. The authigenic Fe-Mn oxyhydroxide fraction was extracted using a gentle reducing cocktail (0.05M hydroxylamine hydrochloride – 15 % acetic acid – 0.03M Na-EDTA, buffered to pH 4 with NaOH) for three hours in a shaker at room temperature.

The seawater origin of the extracted authigenic Fe-Mn oxyhydroxide fraction was ensured by monitoring Al/Pb elemental ratios and by mass balance calculations (Gutjahr et al., 2007). Authigenic Pb in the sediments along the Blake Ridge accounts for 15-40 % of the entire Pb pool present (*i.e.*, the sum of the Fe-Mn oxyhydroxide and terrigenous fraction). By employing a gentle reductive leaching technique, the authigenic Pb isotope signal is not prone to significant contamination from the terrigenous fraction and can be reliably extracted (cf. Poulton and Canfield, 2005).

Separation and purification of Pb from the Fe-Mn oxyhydroxide matrix followed standard procedures (Lugmair and Galer, 1992). The total procedural Pb blank in the Fe-Mn oxyhydroxide fraction was ~ 1 ng and always below 0.35 % of the total Pb concentration. Most Pb isotopic analyses were carried out on a Nu Plasma MC-ICPMS at ETH Zürich applying a Tl-doping procedure (Walder and Furuta, 1993) with a Pb/Tl ~ 4 in the measurement solutions (Table 1). The offset from high precision TIMS Pb isotope data (cf. Thirlwall, 2002) was accounted for by normalising the respective Pb isotope compositions of repeated measurements of NIST SRM981 to Pb isotope ratios of this standard measured by triple spike TIMS ($^{206}Pb/^{204}Pb$ = 16.9405, $^{207}Pb/^{204}Pb$ = 15.4963, $^{208}Pb/^{204}Pb$ = 36.7219) (Galer and Abouchami, 1998). The external reproducibility of the reductive leaching technique was determined from the analyses of 20 duplicate measurements including the complete leaching procedure carried out on samples from cores 51GGC and 12JPC displayed in Table 1. Samples reproduced within 0.032 (1670 ppm) for $^{206}Pb/^{204}Pb$ (best replicate within 52 ppm; average reproducibility: 637 ppm), within 0.012 (765 ppm) for $^{207}Pb/^{204}Pb$ (best replicate within 64 ppm; average reproducibility: 290 ppm), within 0.054 (1380 ppm) for $^{208}Pb/^{204}Pb$ (best replicate within 19 ppm; average reproducibility: 491 ppm), within 0.0012 (1463 ppm) for $^{207}Pb/^{206}Pb$ (best replicate within 6 ppm; average reproducibility: 511 ppm) and within 0.002 (977 ppm) for $^{208}Pb/^{206}Pb$ (best replicate within 15 ppm; average reproducibility: 306 ppm).

Duplicate samples from cores 51GGC and 12JPC were processed chemically and measured separately at least six months later. Six additional samples were processed and analysed at the Bristol Isotope Group of the University of Bristol, UK, using a

ThermoFinnigan Neptune MC-ICPMS (denoted [a] in Table 1). Machine induced mass bias for these additional samples was corrected by standard-sample bracketing normalising the corrected ratios to the triple spike ratios of Galer and Abouchami (1998) for NIST SRM981.

The topmost 360 μm of crust BM1963.897 ('Blake') from the Blake Plateau (30º58'N, 78º30'W, ~850 m depth) was analysed at the University of Bristol using a Thermo Finnigan Neptune MC-ICPMS connected to a NewWave/Merchantek 193nM homogenised ArF excimer laser ablation system. The analytical approach was similar to that of Foster and Vance (2006). All ablation was performed in a pure He environment using a 15 μm diameter aperture, rastering over 0.5 mm lines parallel to growth banding at a speed of 10 μm/sec with a 15 Hz repetition rate and a laser power density of 6-7 J cm^{-2}. Instrumental mass bias was corrected by bracketing groups of seven analyses with analyses of NIST 610 (~400 ppm Pb) using similar analytical conditions (9 J cm^{-2} and a 130 μm spot, 4 Hz) and the NIST 610 Pb isotope ratios of Baker et al. (2004). Eight intercalated analyses of USGS standard NOD-P-1 using an analytical set identical to our unknown samples gave the following results (2σ displayed in ppm, as well as the ratios of Baker et al. (2004) are shown in parentheses; all uncertainties are quoted as 2 sd): $^{206}Pb/^{204}Pb$ = 18.7081 ± 0.0077 (412 ppm) (18.700 ± 0.006), $^{207}Pb/^{204}Pb$ = 15.6363 ± 0.0102 (652 ppm) (15.638 ± 0.003), $^{208}Pb/^{204}Pb$ = 38.6994 ± 0.0220 (568 ppm) (38.697 ± 0.008), $^{207}Pb/^{206}Pb$ = 0.8358 ± 0.0003 (516 ppm) (0.83626 ± 0.00028), $^{208}Pb/^{206}Pb$ = 2.0686 ± 0.0004 (406 ppm) (2.0693 ± 0.0004). The uppermost scan representing the surface of crust 'Blake' was excluded from the interpretations since it was dominated by anthropogenic Pb. Individual results are given in supplementary Table S1.

For the Blake Ridge Fe-Mn oxyhydroxide samples published conventional ^{14}C ages (Keigwin, 2004; Robinson et al., 2005) obtained from planktonic foraminifera for cores 51GGC (n = 12) and 12JPC (n = 3) were transformed into calibrated ages using the marine radiocarbon age calibration Marine04 of Hughen et al. (2004) assuming $\Delta R = 0$. Calibrated ages of other depths in core 12JPC and 51GGC have been linearly interpolated between absolute age tie points. For the age calibration of the analyses performed on crust 'Blake' the $^{10}Be/^{9}Be$ ages determined by Reynolds et al. (1999) have been converted into growth rates (1.89 mm/Myr) for the uppermost 2 Myr.

3. Results

3.1. Lead isotope evolution of seawater from Fe-Mn oxyhydroxides

The authigenic Pb isotope signal extracted from Fe-Mn oxyhydroxides in the sediment cores along the Blake Ridge in the western North Atlantic follow a pronounced and reproducible pattern of rapid change during the transition from the Last Glacial Maximum (LGM) to the Holocene (Figs. 2, 3). All three studied records, whether derived from deep (4250m, 3410m) or intermediate (1790m) water depths, show a rapid increase towards highly radiogenic Pb isotope compositions throughout and beyond the Younger Dryas (Fig. 3) followed by a steady decline towards less radiogenic isotopic compositions during the Holocene, remaining, however, significantly more radiogenic than the glacial values in the youngest samples studied. Since no radiocarbon ages are available for core 31GGC (3410 m) it was not included in Fig. 3. The authigenic Pb isotope record of core 31GGC does, however, show very similar trends to 12JPC and within error it peaks at the same isotopic composition (Table 1, Fig. 2).

The authigenic Pb isotope signal at the deepest location 12JPC was least radiogenic during the LGM and remained so until the Bølling-Allerød interstadial (~14.6 to 12.9 ka BP) (Fig. 3). The Younger Dryas witnessed a rise towards the most radiogenic seawater Pb isotope compositions yet reported for the North Atlantic. The isotopic excursion was larger and of longer duration at the location of deepest core 12JPC than at the intermediate site 51GGC (1790 m). The excursion in these two cores was accompanied by pronounced minima in $^{207}Pb/^{206}Pb$ and $^{208}Pb/^{206}Pb$ (Fig. 3).

The most significant Pb isotopic change seen in deep core 12JPC corresponds to a pronounced shift in the Nd isotope composition (Fig. 3), which traces the establishment of the interglacial mode of deeply ventilating NADW (Gutjahr et al., 2008). The slow decrease towards less radiogenic Pb isotopic compositions observed in 12JPC during the Holocene, however, was not accompanied by corresponding changes in the Nd isotope composition of the same Fe-Mn oxyhydroxide samples.

The trend towards radiogenic Pb isotope compositions recorded by the deep and intermediate depth core sites (here described for $^{206}Pb/^{204}Pb$) clearly already started during the Bølling-Allerød interstadial, but the most significant rise in both water depths occurred during and after the Younger Dryas (Fig. 4). The most radiogenic isotope compositions postdate the Younger Dryas. The rate and duration of change in the Pb isotopic composition is different between the two cores. Core 12JPC shows a relatively steady rise between 14 and ~10 ka BP, whereas site 51GGC recorded the most pronounced change at the onset of the Younger Dryas but the increase only spans a shorter period of time from 14 to 11.2 ka BP. The two core sites experienced

different sedimentation rates during this time interval (cf. Gutjahr et al., 2008). Sedimentation rates in core 51GGC were high throughout the Younger Dryas and the Holocene (Keigwin, 2004), whereas those of core 12JPC decreased significantly with the initiation of Lower NADW ventilation at that site (Haskell and Johnson, 1991; Gutjahr et al., 2008). This change may have had an effect on the temporal resolution of the authigenic Pb isotope signal and renders the intermediate depth core site more reliable in terms of recording the timing of Pb isotope changes *during* the Younger Dryas.

3.2. Long-term Pb isotope evolution in crust 'Blake'

The record of ferromanganese crust 'Blake' shows that the glacial-interglacial Pb isotope variability of the Florida Current only displayed subtle changes over the past 200 kyr (Figs. 1, 5) (e.g. Lynch-Stieglitz et al., 1999; Came et al., 2008). The large Pb isotopic variability observed in crust BM1969.05 from the New England seamounts (Foster and Vance, 2006), which has been located in Upper NADW / Glacial North Atlantic Intermediate Water (GNAIW) during the past 200 kyr, was largely absent in Florida Current waters. The $^{207}Pb/^{206}Pb$ and in particular the $^{208}Pb/^{206}Pb$ records do, however, show some long-term trends of approximately 100 kyr periodicity. The $^{208}Pb/^{206}Pb$ recorded in crust 'Blake' mimics the trends seen in crust BM1969.05 albeit at a smaller amplitude. There is also a tendency towards slightly more radiogenic $^{206}Pb/^{204}Pb$ in crust 'Blake' during the past 100 kyr and low $^{207}Pb/^{206}Pb$ accompanying highest $^{206}Pb/^{204}Pb$, as observed in the sediment cores, is also evident in the ferromanganese crust records.

3.3. $^{207}Pb/^{206}Pb$ and $^{208}Pb/^{206}Pb$ isotope trends

Subtle but distinct seawater Pb isotope differences between the individual core records and the crusts become apparent when comparing the glacial-interglacial $^{207}Pb/^{206}Pb$ and $^{208}Pb/^{206}Pb$ (Fig. 6a). The Fe-Mn oxyhydroxide compositions follow approximately linear trends illustrated by the regression lines for the individual cores. The glacial-interglacial $^{207}Pb/^{206}Pb$ and $^{208}Pb/^{206}Pb$ of the Fe-Mn oxyhydroxides are shown together with laser ablation data of Foster and Vance (2006) for crust BM1969.05 and crust 'Blake' analysed here. There is good agreement between the two different seawater archives. The glacial-interglacial $^{207}Pb/^{206}Pb$ and $^{208}Pb/^{206}Pb$ compositions of deepest core 12JPC match best those of ferromanganese crust BM1969.05, which grew in 1830 m water depth, whereas intermediate core 51GGC correlates well with crust 'Blake', which grew in waters of the Florida Current on Blake Plateau. The record of core 31GGC from 3410 m water depth is intermediate between the compositions of the other two cores. The spatial and temporal trends can best be illustrated by only displaying individual compositions during the LGM, after the Younger Dryas and during the late Holocene, such as shown in Figure 6b. Both $^{208}Pb/^{206}Pb$ and $^{207}Pb/^{206}Pb$ are highest during the LGM and lowest after the Younger Dryas. Present-day ratios fall between these end-member compositions.

4. Discussion

The trends seen in the Pb isotope records of past seawater over termination 1 were governed by a number of potential processes including (a) changes in the continental sources available for chemical weathering; (b) changes in the Pb-specific incongruent weathering signal due to enhanced availability of fresh glacially eroded sediments; (c) changes in the routing of fresh water runoff; and (d) changes in the vigour and

location of the western boundary undercurrent. These processes will be discussed in the following.

For North Atlantic settings, it is essential to first investigate the importance of a fifth process, which is the presence and potential influence of IRD since the reductive leaching protocol applied here aims to dissolve authigenic Fe-Mn oxyhydroxides from marine sediments. If present, hematite-stained IRD could dominate the extracted authigenic Pb isotope signal (Poulton and Canfield, 2005); however, leaching of IRD is not an issue for Blake Ridge sediments. In a multi-proxy study covering MIS 3, Vautravers et al. (2004) found negligible amounts of IRD at ODP Site 1060 (3480 m), supporting the conclusion that the Blake Ridge is located about 2º south of the southernmost location at which evidence for glacial iceberg discharge has been reported (Keigwin and Boyle, 1999). This renders the extracted seawater Pb isotope signal robust against partial leaching of terrigenous Fe-Mn oxyhydroxides.

4.1. Regional deglacial Pb isotopic trends

The seawater Pb isotopic signal recorded in both deep (4250 m) and intermediate (1790 m) water depth consistently shows the least radiogenic compositions during or even slightly before the LGM, with no significant excursion towards radiogenic compositions prior to the mid-Bølling-Allerød (Figs. 3, 4). The most pronounced shift occurred during the Younger Dryas, peaking in the subsequent transition to the Holocene. Likewise, ferromanganese crust BM1969.05 situated in Upper NADW / GNAIW shows a pronounced change over the past 30 kyr (grey box in Fig. 5). In contrast, the Pb isotopic composition of crust ‘Blake’ that recorded the isotopic variability of the Florida Current, remained almost unchanged during this time interval. This diverging pattern strongly suggests that the highly radiogenic Pb flux

that has been recorded in the Fe-Mn oxyhydroxides at the Blake Ridge was advected from the north.

The most significant change in the deep core 12JPC coincided with the establishment of Lower NADW ventilation along the deep Blake Ridge (Fig. 3) (Gutjahr et al., 2008). The relatively radiogenic Nd isotope compositions (ε_{Nd} ~ -10.5) observed in the deep core 12JPC until the Younger Dryas (Fig. 3) reflect the absence of Lower NADW (modern NADW: ε_{Nd} ~ -13.5) along the deeper Blake Ridge throughout the deglaciation. The concurrent major change in the authigenic Nd and Pb isotope records over the Younger Dryas at site 12JPC (Figs. 3, 4) therefore most likely reflect an invigorated overturning circulation of the western boundary undercurrent along the deeper Blake Ridge.

Core site 51GGC in 1790 m water depth was always located within Upper NADW / GNAIW (Boyle and Keigwin, 1987; Marchitto et al., 1998; McManus et al., 2004; Robinson et al., 2005; Came et al., 2008). It experienced high sedimentation rates throughout the deglaciation (Keigwin, 2004) and, as opposed to the deep core sites, should have recorded a northern-sourced signal throughout the entire period of time between 14 kyr and the Holocene. Yet the extracted Pb isotope signal of this site is expected to represent a mixed authigenic signal consisting of (a) the local intermediate bottom water mass Pb isotope signal and (b) contributions from local shallow water sources. This suggestion is based on the extracted authigenic Nd isotope composition from this core, which does not match expected upper NADW compositions at any time since the LGM (see discussion in Gutjahr et al., 2008). The authigenic Nd isotope signal at intermediate depths (core 51GGC) during the

deglacial and Holocene is very similar to the bottom water composition of the overlying Florida Current.

The earlier observation that the extracted *in situ* intermediate depth Fe-Mn oxyhydroxide signal is to some extent offset towards surface water compositions is supported by the authigenic Pb isotope data presented here from the same Fe-Mn oxyhydroxide samples. The linear regression lines included in Figure 6 reveal systematic differences in the authigenic $^{208}Pb/^{206}Pb$ and $^{207}Pb/^{206}Pb$ isotope compositions at different depths along the Blake Ridge. The glacial-interglacial Pb isotope compositions for crust 'Blake', recording a Florida Current bottom water signal, bear similarities to those of core 51GGC, whereas the Pb isotope ratios of deeper core sites 31GGC and 12JPC agree with those GNAIW/NADW Pb isotope compositions seen in ferromanganese crust BM1969.05 (Fig. 6a) (Foster and Vance, 2006). On the other hand, the most radiogenic Pb isotope compositions recorded in 51GGC differ from those seen in crust 'Blake' (significantly more radiogenic Pb isotopic compositions leading to lower $^{208}Pb/^{206}Pb$ and $^{207}Pb/^{206}Pb$ in Fig. 6).

Within the coarse-resolution Pb isotope record of crust 'Blake', there are no significant variations during the deglaciation (Fig. 5) whereas core 51GGC shows a clear trend towards radiogenic compositions similar to 12JPC during the Younger Dryas (Fig. 4). This suggests that, although the authigenic Pb isotope record of 51GGC represents a mixed signal partially offset towards the Florida Current Pb isotope compositions (Fig. 6), the radiogenic deglacial Pb isotope excursion is controlled by a northern-sourced signal (Figs. 4, 5). This implies that the GNAIW

ventilating site 51GGC at the Blake Ridge did not carry a distinctly radiogenic Pb isotope signal over most of the deglaciation until the mid-Bølling-Allerød (Figs. 3, 4).

4.2. Incipient chemical weathering and the Pb isotopic runoff signal

In mid- to high-latitudinal settings, such as on the North American shield during the Pleistocene, the Pb isotope runoff signal during an 'ice house' climate is expected to be primarily controlled by climate as opposed to source rock composition (von Blanckenburg and Nägler, 2001). During the glacial cycles of the Pleistocene the Laurentide ice sheet created extensive quantities of fresh glacially eroded rock substrate (Bell and Laine, 1985). This material was not significantly chemically weathered during glacials since large areas of North America were covered by ice. Deglacial warming and the recurring large-scale retreat of the Laurentide ice sheet during glacial terminations should then have led to highly elevated cation fluxes (e.g. Vance et al., 2009). As a consequence, the onset and intensification of chemical weathering of previously glaciated terrains would also have led to the preferential release of highly radiogenic Pb (Harlavan et al., 1998; Foster and Vance, 2006).

Due to this mechanism deep core site 12JPC deserves particular attention since it represents the purest Pb isotope signal of higher northern latitudes (i.e. advected to the Blake Ridge within NADW) during the late deglaciation and the Holocene (see section 4.1). Authigenic Pb isotope compositions peak during the early Holocene, coinciding with the climatic optimum and the final disappearance of the Laurentide ice sheet (Licciardi et al., 1998). Lead isotope compositions have become continuously less radiogenic over the course of the Holocene but remained significantly more radiogenic than during the last glacial (Fig. 3). From the

399 apparently asymptotic trend of the late Holocene Pb isotope compositions in core
400 12JPC (Fig. 3), it could be argued that the present-day chemical weathering fluxes are
401 still levelling out towards a long-term steady state. This argument is supported by the
402 longer-term trends of the Pb isotope records of the ferromanganese crusts (Fig. 7).
403 The Pb flux into the western North Atlantic became increasingly more radiogenic
404 over the past 1.8 Myr (Fig. 7) (Burton et al., 1997; O'Nions et al., 1998; Reynolds et
405 al., 1999). This trend implies that more glacially eroded fresh rock substrate was
406 created throughout the Pleistocene glacial periods (Peizhen et al., 2001) than could be
407 chemically weathered during the relatively short interspersed interglacials (cf. Vance
408 et al., 2009).
409
410 Although it is impossible to trace the continental source areas of the advected Pb by
411 means of the extracted authigenic Pb isotope composition in Blake Ridge sediments
412 due to the fractionation caused by incongruent weathering processes, it is possible to
413 calculate a bulk average $^{207}Pb/^{206}Pb$ age for the continental source area that supplied
414 dissolved Pb to the three core sites along the Blake Ridge (Fig. 8). The age obtained
415 from all three cores (1.48 ± 0.26 Ga) for the continental source area is identical within
416 error to the ages obtained by van de Flierdt et al. (2002) for Pb isotope data on crusts
417 ALV539 (1.68 +0.17 -0.20 Ga) and BM1969.05 to the North of the Blake Ridge (1.30
418 +0.31 -0.39 Ga). The age estimates given by Foster and Vance (2006) for these two
419 crusts based on their laser ablation Pb isotope records of the past 500 kyr are
420 significantly older (2.0 to 2.5 Gyr) and may indicate weathering contributions from
421 older source rocks for this period. The average bulk source age obtained from the Fe-
422 Mn oxyhydroxides presented here suggest that a significant portion of the Pb supplied

to the Blake Ridge were derived from the Proterozoic cratonic areas in the interior of northern North America and/or areas bordering the Labrador Sea.

5. Conclusions

The seawater Pb isotope evolution recorded by sediment cores in intermediate and deep waters along the Blake Ridge in the North Atlantic underwent substantial variations during termination 1. The general pattern seen in all water depths is a shift from unradiogenic Pb isotope compositions during the last glacial to very radiogenic compositions throughout and after the Younger Dryas, followed by a continuous decline towards somewhat less radiogenic Pb isotope compositions today. The spatial and temporal Pb isotope trends in the western North Atlantic were governed by provenance, changes in deep ocean circulation, and by climatically induced changes in weathering regime.

Our data suggest that fresh rock substrate, physically eroded during the last glacial cycle, incongruently released large quantities of radiogenic Pb during incipient and continued chemical weathering following the retreat of the Laurentide ice sheet and accompanying proglacial lake formation on the North American continent. North Atlantic Deep Water that ventilated the Lower Blake Ridge after the Younger Dryas supplied a continent-derived highly radiogenic Pb signal throughout the Holocene. This signal has been a direct function of elevated chemical weathering rates in recently deglaciated terranes in North America.

Our records indicate that the continental Pb input into the North Atlantic was significantly reduced during the Last Glacial Maximum, and that long-term Pb isotope

trends towards more radiogenic compositions recorded in ferromanganese crusts are likely dominated by short-lived interglacial and interstadial Pb isotope signals during otherwise prevailing ice-house conditions, implying that the majority of continental radiogenic Pb was supplied to the North Atlantic during interglacials. In the vicinity of the Blake Ridge Glacial North Atlantic Intermediate Water likely did not carry a distinctly radiogenic Pb isotope signal over most of the deglaciation until the mid-Bølling-Allerød.

Acknowledgments

Funding for this project was provided by grant TH-12 02-2 of ETH Zurich. We acknowledge Felix Oberli, Claudine Stirling, Helen Williams, Sarah Woodland, Mark Rehkämper, Heiri Baur, Urs Menet, Donat Niederer, Bruno Rütsche and Anreas Süsli for their help in keeping the MC-ICPMS running smoothly and their support in the clean labs and with the computers. Chris Coath within the Bristol Isotope Group maintains an excellent machine support. Gavin Foster is acknowledged for providing assistance with the laser ablation Pb isotopic measurements. This manuscript benefited from discussions with Kirsty Crocket, Tina van de Flierdt, Gavin Foster and Ben Reynolds. Derek Vance provided further valuable comments. The British Natural History Museum and Sune Nielsen are acknowledged for providing a sub-sample of crust ‘Blake’. Ellen Martin and Sidney Hemming provided valuable comments, which improved an earlier version of the manuscript. Peggy Delaney is acknowledged for editorial handling, as well as further constructive criticism.

References

Abouchami, W., Goldstein, S.L., 1995. A lead isotopic study of circum-Antarctic manganese nodules. Geochim. Cosmochim. Acta 59 (9), 1809-1820.

Abouchami, W., Galer, S.J.G., Koschinsky, A., 1999. Pb and Nd isotopes in NE Atlantic Fe-Mn crusts: Proxies for trace metal paleosources and paleocean circulation. Geochim. Cosmochim. Acta 63 (10), 1489-1505.

Anderson, S.P., Drever, J.I., Frost, C.D., Holden, P., 2000. Chemical weathering in the foreland of a retreating glacier. Geochim. Cosmochim. Acta 64 (7), 1173-1189.

Baker, J., Peate, D., Waight, T., Meyzen, C., 2004. Pb isotopic analysis of standards and samples using a Pb-207-Pb-204 double spike and thallium to correct for mass bias with a double-focusing MC-ICP-MS. Chem. Geol. 211 (3-4), 275-303.

Bell, M., Laine, E.P., 1985. Erosion of the Laurentide region of North America by glacial and glaciofluvial processes. Quat. Res. 23 (2), 154-174.

Boyle, E.A., Keigwin, L.D., 1987. North Atlantic thermohaline circulation during the past 20,000 years linked to high-latitude surface temperature. Nature 330 (6143), 35-40.

Burton, K.W., Ling, H.-F., O'Nions, R.K., 1997. Closure of the Central American Isthmus and its effect on deep-water formation in the North Atlantic. Nature 386, 382-385.

Came, R.E., Oppo, D.W., Curry, W.B., Lynch-Stieglitz, J., 2008. Deglacial variability in the surface return flow of the Atlantic meridional overturning circulation. Paleoceanography 23, Art. No.: PA1217.

492 Christensen, J.N., Halliday, A.N., Godfrey, L.V., Hein, J.R., Rea, D.K., 1997. Climate
493 and ocean dynamics and the lead isotopic records in Pacific ferromanganese crusts.
494 Science 277, 913-918.

495 Clark, P.U., Archer, D., Pollard, D., Blum, J.D., Rial, J.A., Brovkin, V., Mix, A.C.,
496 Pisias, N.G., Roy, M., 2006. The middle Pleistocene transition: characteristics,
497 mechanisms, and implications for long-term changes in atmospheric pCO_2. Quat. Sci.
498 Rev. 25 (23-24), 3150-3184.

499 Craig, H., Krishnas.S, Somayaju.Bl, 1973. Pb-210 - Ra-226 - radioactive
500 disequilibrium in the deep sea. Earth Planet. Sci. Lett. 17 (2), 295-305.

501 Curry, W.B., Oppo, D.W., 2005. Glacial water mass geometry and the distribution of
502 delta C-13 of ΣCO_2 in the western Atlantic Ocean. Paleoceanography 20 (1), Art. No.:
503 PA1017.

504 Dyke, A.S., Andrews, J.T., Clark, P.U., England, J.H., Miller, G.H., Shaw, J.,
505 Veillette, J.J., 2002. The Laurentide and Innuitian ice sheets during the Last Glacial
506 Maximum. Quat. Sci. Rev. 21 (1-3), 9-31.

507 Erel, Y., Blum, J.D., Roueff, E., Ganor, J., 2004. Lead and strontium isotopes as
508 monitors of experimental granitoid mineral dissolution. Geochim. Cosmochim. Acta
509 68 (22), 4649-4663.

510 Foster, G.L., Vance, D., 2006. Negligible glacial-interglacial variation in continental
511 chemical weathering rates. Nature 444 (7121), 918-921.

512 Frank, M., O'Nions, R.K., Hein, J.R., Banakar, V.K., 1999a. 60 Myr records of major
513 elements and Pb-Nd isotopes from hydrogenous ferromanganese crusts:

514 reconstruction of seawater paleochemistry. Geochim. Cosmochim. Acta 63 (11-12),
515 1689-1708.

516 Frank, M., Reynolds, B.C., O'Nions, R.K., 1999b. Nd and Pb isotopes in Atlantic and
517 Pacific water masses before and after closure of the Panama gateway. Geology 27
518 (12), 1147-1150.

519 Frank, M., Whiteley, N., Kasten, S., Hein, J.R., O'Nions, R.K., 2002. North Atlantic
520 Deep Water export to the Southern Ocean over the past 14 Myr: Evidence from Nd
521 and Pb isotopes in ferromanganese crusts. Paleoceanography 17 (2), Art. No.: 1022.

522 Galer, S.J.G., Abouchami, W., 1998. Practical application of lead triple spiking for
523 correction of instrumental mass discrimination. Min. Mag. 62A, 491–492.

524 Gislason, S.R., Oelkers, E.H., Eiriksdottir, E.S., Kardjilov, M.I., Gisladottir, G.,
525 Sigfusson, B., Snorrason, A., Elefsen, S., Hardardottir, J., Torssander, P., Oskarsson,
526 N., 2009. Direct evidence of the feedback between climate and weathering. Earth
527 Planet. Sci. Lett. 277 (1-2), 213-222.

528 Gutjahr, M., Frank, M., Stirling, C.H., Klemm, V., van de Flierdt, T., Halliday, A.N.,
529 2007. Reliable extraction of a deepwater trace metal isotope signal from Fe-Mn
530 oxyhydroxide coatings of marine sediments. Chem. Geol. 242 (3-4), 351-370.

531 Gutjahr, M., Frank, M., Stirling, C.H., Keigwin, L.D., Halliday, A.N., 2008. Tracing
532 the Nd isotope evolution of North Atlantic Deep and Intermediate Waters in the
533 western North Atlantic since the Last Glacial Maximum from Blake Ridge sediments.
534 Earth Planet. Sci. Lett. 266 (1-2), 61-77.

535 Haley, B.A., Frank, M., Spielhagen, R.F., Fietzke, J., 2008. Radiogenic isotope record
536 of Arctic Ocean circulation and weathering inputs of the past 15 million years.
537 Paleoceanography 23, Art. No.: PA1S13.

538 Harlavan, Y., Erel, Y., Blum, J.D., 1998. Systematic changes in lead isotopic
539 composition with soil age in glacial granitic terrains. Geochim. Cosmochim. Acta 62
540 (1), 33-46.

541 Harlavan, Y., Erel, Y., 2002. The release of Pb and REE from granitoids by the
542 dissolution of accessory phases. Geochim. Cosmochim. Acta 66 (5), 837-848.

543 Haskell, B.J., Johnson, T.C., 1991. Fluctuations in deep western North Atlantic
544 circulation on the Blake Outer Ridge during the last deglaciation. Paleoceanography
545 6, 21-31.

546 Hemming, S.R., 2004. Heinrich events: Massive late pleistocene detritus layers of the
547 North Atlantic and their global climate imprint. Rev. Geophys. 42 (1), Art. No.:
548 RG1005.

549 Henderson, G.M., Maier-Reimer, E., 2002. Advection and removal of ^{210}Pb and stable
550 Pb isotopes in the oceans: a general circulation model study. Geochim. Cosmochim.
551 Acta 66 (2), 257-272.

552 Hughen, K.A., Baillie, M.G.L., Bard, E., Beck, J.W., Bertrand, C.J.H., Blackwell,
553 P.G., Buck, C.E., Burr, G.S., Cutler, K.B., Damon, P.E., Edwards, R.L., Fairbanks,
554 R.G., Friedrich, M., Guilderson, T.P., Kromer, B., McCormac, G., Manning, S.,
555 Ramsey, C.B., Reimer, P.J., Reimer, R.W., Remmele, S., Southon, J.R., Stuiver, M.,
556 Talamo, S., Taylor, F.W., van der Plicht, J., Weyhenmeyer, C.E., 2004. Marine04
557 marine radiocarbon age calibration, 0–26 cal kyr BP. Radiocarbon 46, 1059-1086.

558 Imbrie, J.D., Hays, J.D., Martinson, D.G., McIntyre, A., Mix, A.C., Morley, J., Pisias,
559 N.G., Prell, W.L., Shackleton, N.J., 1984. The orbital theory of Pleistocene climate:
560 support from a revised chronology of the marine $\delta^{18}O$ record, in: A.L. Berger, J.
561 Imbrie, J.D. Hays, G. Kukla, E. Saltzman, (Eds.), Milankovitch and Climate. Reidel,
562 Dordrecht, 269–305.

563 Joyce, J.E., Tjalsma, L.R.C., Prutzman, J.M., 1993. North American glacial meltwater
564 history for the past 2.3 Myr – oxygen isotope evidence from the Gulf of Mexico.
565 Geology 21 (6), 483-486.

566 Keigwin, L.D., Boyle, E.A., 1999. Surface and deep ocean variability in the northern
567 Sargasso Sea during marine isotope stage 3. Paleoceanography 14 (2), 164-170.

568 Keigwin, L.D., 2004. Radiocarbon and stable isotope constraints on Last Glacial
569 Maximum and Younger Dryas ventilation in the western North Atlantic.
570 Paleoceanography 19 (4), Art. No.: PA4012.

571 Licciardi, J.M., Clark, P.U., Jenson, J.W., Macayeal, D.R., 1998. Deglaciation of a
572 soft-bedded Laurentide Ice Sheet. Quat. Sci. Rev. 17 (4-5), 427-448.

573 Lugmair, G.W., Galer, S.J.G., 1992. Age and isotopic relationships among the
574 angrites Lewis Cliff 86010 and Angra dos Reis. Geochim. Cosmochim. Acta 56 (4),
575 1673-1694.

576 Lynch-Stieglitz, J., Curry, W.B., Slowey, N., 1999. Weaker Gulf Stream in the
577 Florida straits during the last glacial maximum. Nature 402 (6762), 644-648.

578 Lynch-Stieglitz, J., Adkins, J.F., Curry, W.B., Dokken, T., Hall, I.R., Herguera, J.C.,
579 Hirschi, J.J.M., Ivanova, E.V., Kissel, C., Marchal, O., Marchitto, T.M., McCave,

I.N., McManus, J.F., Mulitza, S., Ninnemann, U., Peeters, F., Yu, E.-F., Zahn, R., 2007. Atlantic meridional overturning circulation during the Last Glacial Maximum. Science 316 (5821), 66-69.

Marchitto, T.M., Curry, W.B., Oppo, D.W., 1998. Millennial-scale changes in North Atlantic circulation since the last glaciation. Nature 393 (6685), 557-561.

Marshall, S.J., Clarke, G.K.C., 1999. Modelling North American freshwater runoff through the last glacial cycle. Quat. Res. 52 (3), 300-315.

Marshall, S.J., Clark, P.U., 2002. Basal temperature evolution of North American ice sheets and implications for the 100-kyr cycle. Geophys. Res. Lett. 29 (24), Art. No.: 2214.

McManus, J.F., Francois, R., Gherardi, J.M., Keigwin, L.D., Brown-Leger, S., 2004. Collapse and rapid resumption of Atlantic meridional circulation linked to deglacial climate changes. Nature 428 (6985), 834-837.

Millot, R., Gaillardet, J., Dupré, B., Allègre, C.J., 2003. Northern latitude chemical weathering rates: Clues from the Mackenzie River Basin, Canada. Geochim. Cosmochim. Acta 67 (7), 1305-1329.

NGRIP Members, 2004. High-resolution record of Northern Hemisphere climate extending into the last interglacial period. Nature 431 (7005), 147-151.

O'Nions, R.K., Frank, M., von Blanckenburg, F., Ling, H.F., 1998. Secular variation of Nd and Pb isotopes in ferromanganese crusts from the Atlantic, Indian and Pacific Oceans. Earth Planet. Sci. Lett. 155 (1-2), 15-28.

601 Peizhen, Z., Molnar, P., Downs, W.R., 2001. Increased sedimentation rates and grain
602 sizes 2-4 Myr ago due to the influence of climate change on erosion rates. Nature 410
603 (6831), 891-897.

604 Poulton, S.W., Canfield, D.E., 2005. Development of a sequential extraction
605 procedure for iron: implications for iron partitioning in continentally derived
606 particulates. Chem. Geol. 214 (3-4), 209-221.

607 Reynolds, B.C., Frank, M., O'Nions, R.K., 1999. Nd- and Pb-isotope time series from
608 Atlantic ferromanganese crusts: implications for changes in provenance and
609 paleocirculation over the last 8 Myr. Earth Planet. Sci. Lett. 173 (4), 381-396.

610 Robinson, L.F., Adkins, J.F., Keigwin, L.D., Southon, J., Fernandez, D.P., Wang,
611 S.L., Scheirer, D.S., 2005. Radiocarbon variability in the western North Atlantic
612 during the last deglaciation. Science 310 (5753), 1469-1473.

613 Schaule, B.K., Patterson, C.C., 1981. Lead concentrations in the northeast Pacific -
614 evidence for global anthropogenic perturbations. Earth Planet. Sci. Lett. 54 (1), 97-
615 116.

616 Steffensen, J.P., Andersen, K.K., Bigler, M., Clausen, H.B., Dahl-Jensen, D., Fischer,
617 H., Goto-Azuma, K., Hansson, M., Johnsen, S.J., Jouzel, J., Masson-Delmotte, V.,
618 Popp, T., Rasmussen, S.O., Rothlisberger, R., Ruth, U., Stauffer, B., Siggaard-
619 Andersen, M.-L., Sveinbjornsdottir, A.E., Svensson, A., White, J.W.C., 2008. High-
620 resolution Greenland ice core data show abrupt climate change happens in few years.
621 Science 321 (5889), 680-684.

622 Thirlwall, M.F., 2002. Multicollector ICP-MS analysis of Pb isotopes using a ^{207}Pb-
623 ^{204}Pb double spike demonstrates up to 400 ppm/amu systematic errors in Tl-
624 normalization. Chem. Geol. 184 (3-4), 255-279.

625 Tranter, M., Huybrechts, P., Munhoven, G., Sharp, M.J., Brown, G.H., Jones, I.W.,
626 Hodson, A.J., Hodgkins, R., Wadham, J.L., 2002. Direct effect of ice sheets on
627 terrestrial bicarbonate, sulphate and base cation fluxes during the last glacial cycle:
628 minimal impact on atmospheric CO_2 concentrations. Chem. Geol. 190 (1-4), 33-44.

629 van de Flierdt, T., Frank, M., Lee, D.C., Halliday, A.N., 2002. Glacial weathering and
630 the hafnium isotope composition of seawater. Earth Planet. Sci. Lett. 198 (1-2), 167-
631 175.

632 Vance, D., Teagle, D.A.H., Foster, G.L., 2009. Variable Quaternary chemical
633 weathering fluxes and imbalances in marine geochemical budgets. Nature 458 (7237),
634 493-496.

635 Vautravers, M.J., Shackleton, N.J., Lopez-Martinez, C., Grimalt, J.O., 2004. Gulf
636 Stream variability during marine isotope stage 3. Paleoceanography 19 (2), Art. No.:
637 PA2011.

638 von Blanckenburg, F., Onions, R.K., Hein, J.R., 1996. Distribution and sources of
639 pre-anthropogenic lead isotopes in deep ocean water from Fe-Mn crusts. Geochim.
640 Cosmochim. Acta 60 (24), 4957-4963.

641 von Blanckenburg, F., Nägler, T.F., 2001. Weathering versus circulation-controlled
642 changes in radiogenic isotope tracer composition of the Labrador Sea and North
643 Atlantic Deep Water. Paleoceanography 16 (4), 424-434.

644 Walder, A.J., Furuta, N., 1993. High-precision lead-isotope ratio measurement by
645 inductively-coupled plasma multiple collector mass-spectrometry. Anal. Sci. 9 (5),
646 675-680.

647 West, A.J., Galy, A., Bickle, M., 2005. Tectonic and climatic controls on silicate
648 weathering. Earth Planet. Sci. Lett. 235 (1-2), 211-228.

649 White, A.F., Heinrich, D.H., Karl, K.T., 2003. Natural weathering rates of silicate
650 minerals, Treat. Geochem., Pergamon, Oxford, 133-168.

Figure Captions

Figure 1. Core locations along the Blake Ridge in the western North Atlantic. Trajectories of the schematic flow paths of the Florida current in water depths above 1000 m, and the Western Boundary Undercurrent (WBUC) transporting North Atlantic Deep Water southward are indicated. Also shown are the sampling locations of ferromanganese crusts BM1969.05 from the New England seamounts (Reynolds et al., 1999; Foster and Vance, 2006), as well as crust 'Blake' analysed here.

Figure 2. Authigenic Pb isotope evolution as recorded in Fe-Mn oxyhydroxides from drift sediments along the Blake Ridge, plotted against depth in cores. Arrows in the bottom panels of (a) and (c) highlight depths in core for which radiocarbon ages from planktonic foraminifera are available. Since no radiocarbon dates are available for core 31GGC it is not included in Fig. 3. Radiocarbon ages and the oxygen isotope stratigraphy are from Keigwin (2004) with one additional radiocarbon age for 12JPC from Robinson et al. (2005). White diamonds in the upper panel highlight sampled depths for authigenic Pb isotope compositions. Yellow diamonds in the lower panels highlight individual measurement results for sections in which duplicates were produced (see also Table 1).

Figure 3. Deep and intermediate depth authigenic Pb isotope evolution from Blake Ridge Fe-Mn oxyhydroxides represented by cores 12JPC (4250 m) and 51GGC (1790 m) over the past 28 kyr. The shaded areas highlight the Younger Dryas (YD) and the Last Glacial Maximum (LGM). The neodymium isotope signal of the same core sections is shown in the lower panel (Gutjahr et al., 2008). See text for discussion.

675

676 **Figure 4.** Deep and intermediate water $^{206}Pb/^{204}Pb$ evolution along the Blake Ridge
677 in the western North Atlantic during the deglaciation and the transition to the
678 Holocene, plotted together with the NGRIP oxygen isotope record (NGRIP Members,
679 2004).

680

681 **Figure 5.** Comparison of the long-term deep water Pb isotope evolution of
682 ferromanganese crusts BM1969.05 (1829 m, solid circles, Foster and Vance, 2006)
683 and crust 'Blake' (850 m, this study, open circles) over the past 200 kyr. In the right
684 panel the Pb isotope evolution of 'Blake' is plotted individually at an expanded scale.
685 Error bars represent the external reproducibility of six laser ablation measurements
686 carried out on pressed USGS ferromanganese powder NOD-P-1.

687

688 **Figure 6.** $^{207}Pb/^{206}Pb$ versus $^{208}Pb/^{206}Pb$ for Fe-Mn oxyhydroxide fractions in the
689 three sediment cores and two ferromanganese crusts. Linear regression lines and
690 coefficients are displayed for a better distinction of the Pb isotope trends in the Fe-Mn
691 oxyhydroxide-derived data. The two Fe-Mn crust records represent laser ablation
692 results of ferromanganese crust BM1969.05 (1829 m) published by Foster and Vance
693 (2006) and new laser ablation data from crust 'Blake' (850 m) (this study). (b)
694 Schematic presentation for individual LGM, post-Younger Dryas and late Holocene
695 Pb isotopic compositions. Symbols in (b) are the same as in (a).

696

697 **Figure 7.** Comparison of the deep water Pb isotope evolution of crust 'Blake', as
698 obtained via solution work by Reynolds et al. (1999) and the higher resolution laser
699 ablation data presented here. The $^{206}Pb/^{204}Pb$ isotope composition of the Florida

700 Current became increasingly more radiogenic in the course of the Pleistocene. This
701 feature, in context with the short-term Pb isotopic changes, suggests that more rock
702 substrate is crushed during glacial erosion throughout glacial cycles than can be
703 removed during intervening relatively short interglacial chemical weathering.
704
705 **Figure 8.** Bulk average $^{207}Pb/^{206}Pb$ age calculated for the extracted Fe-Mn
706 oxyhydroxide fraction of all three cores from the Blake Ridge presented in Fig. 2 and
707 listed in Table 1.

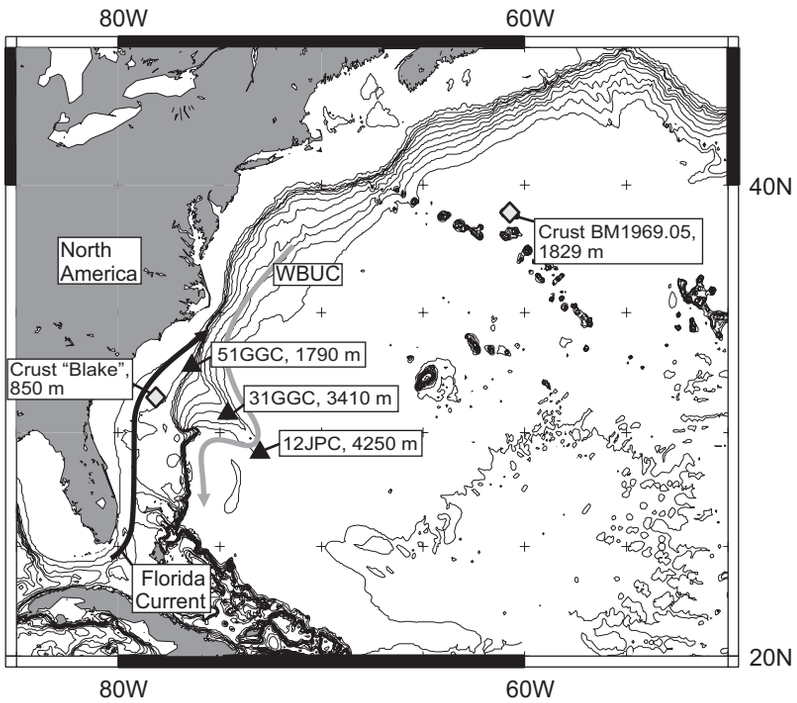

Figure 1 - Gutjahr et al.

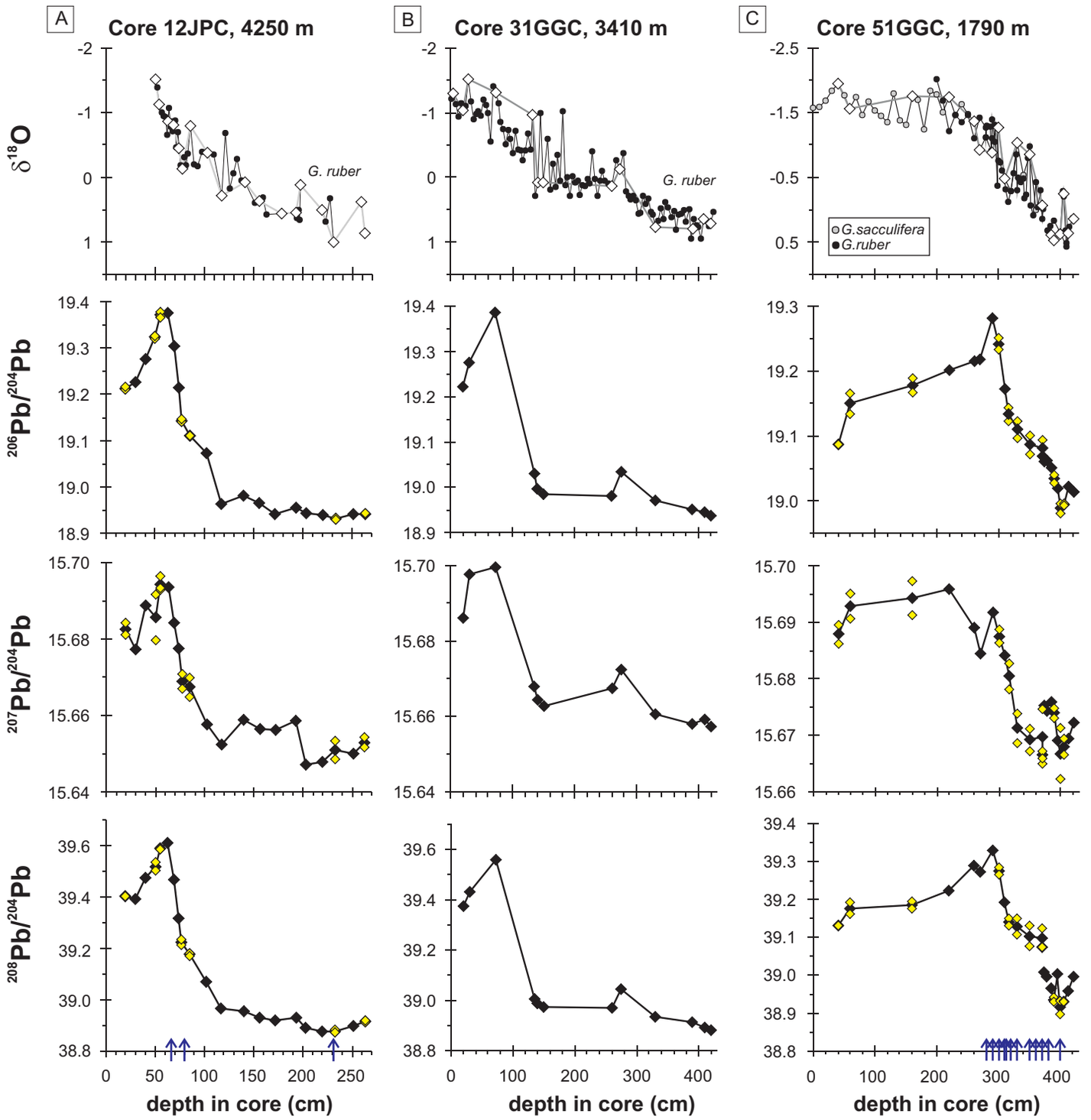

Figure 2 - Gutjahr et al.

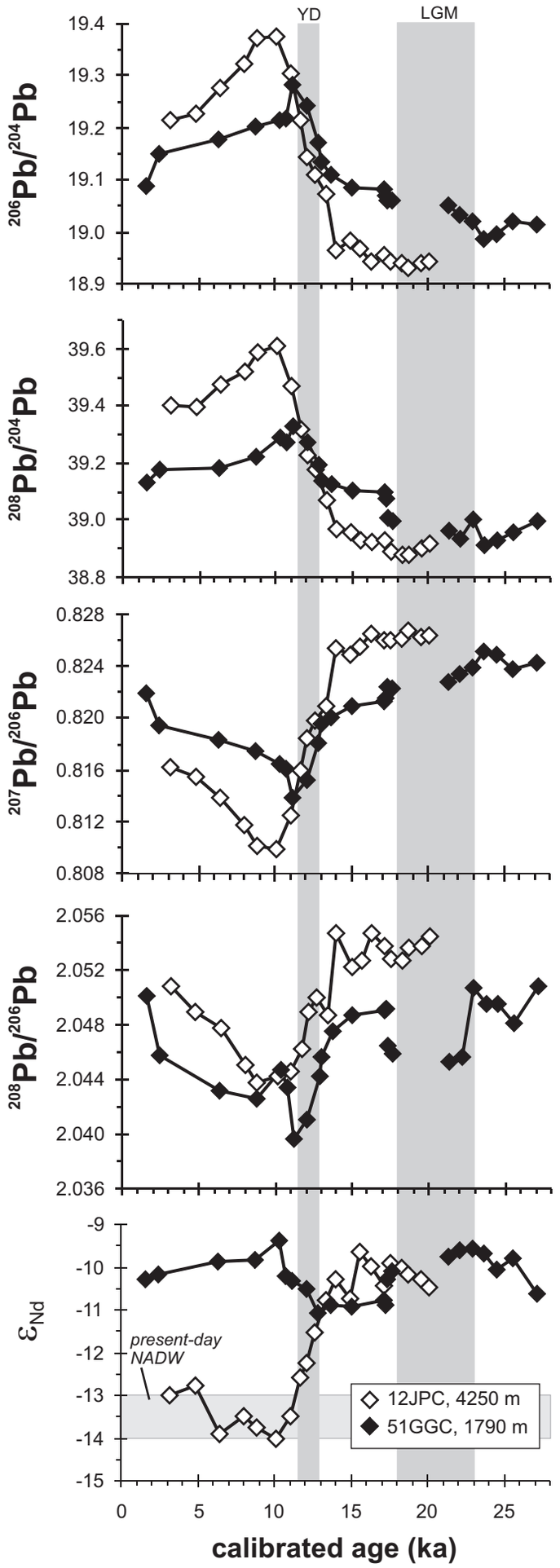

Figure 3 - Gutjahr et al.

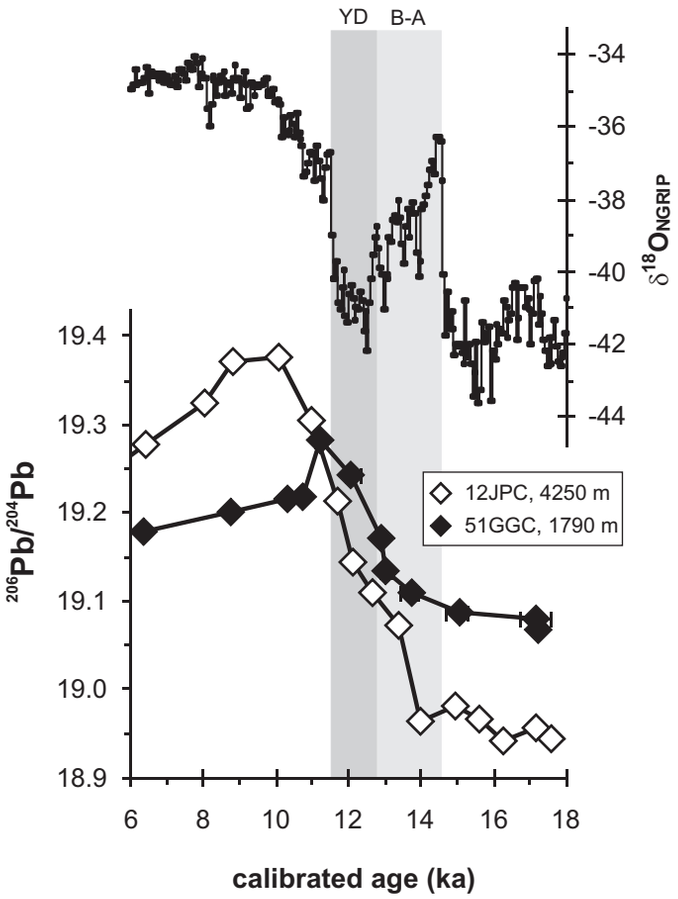

Figure 4 - Gutjahr et al.

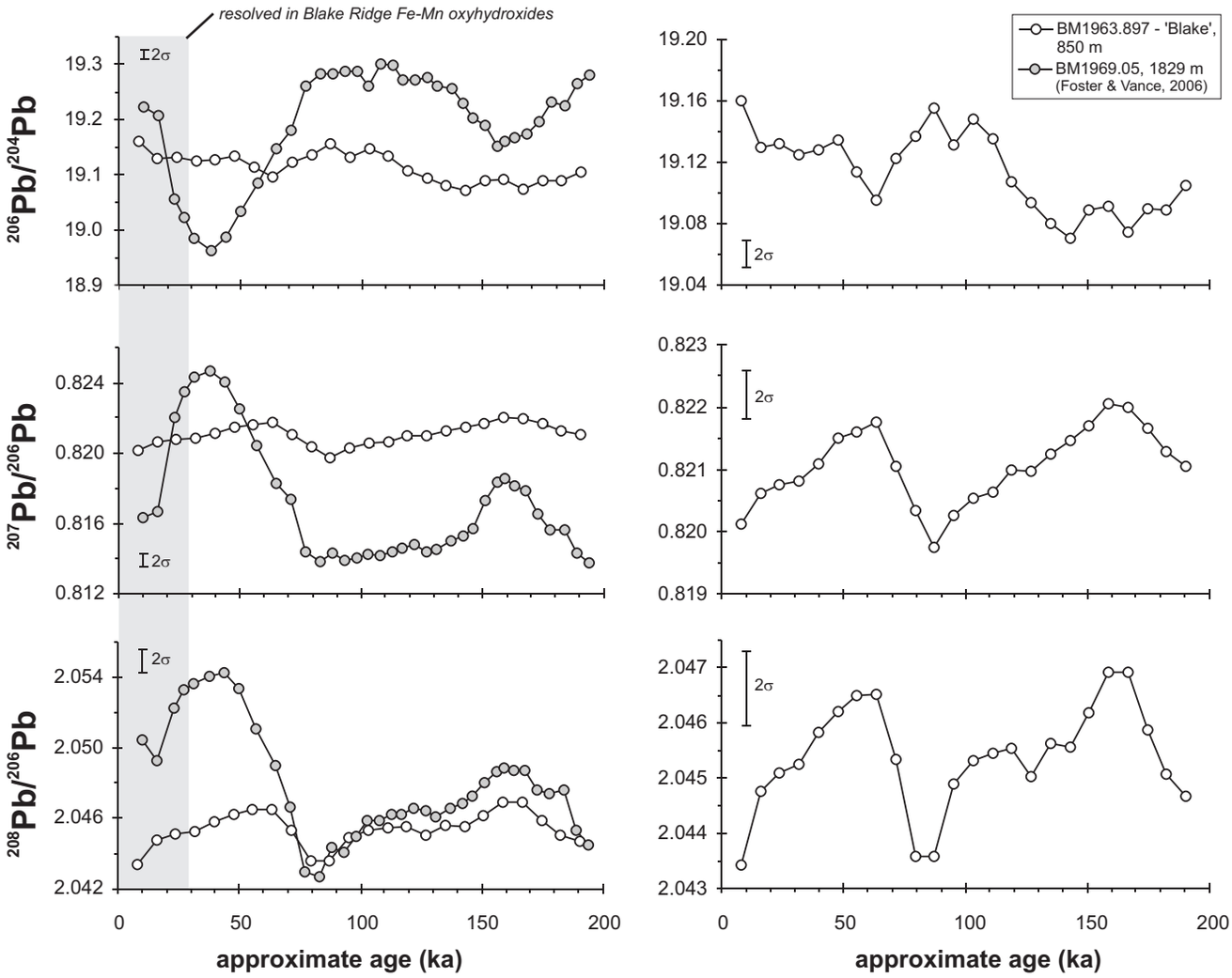

Figure 5 - Gutjahr et al.

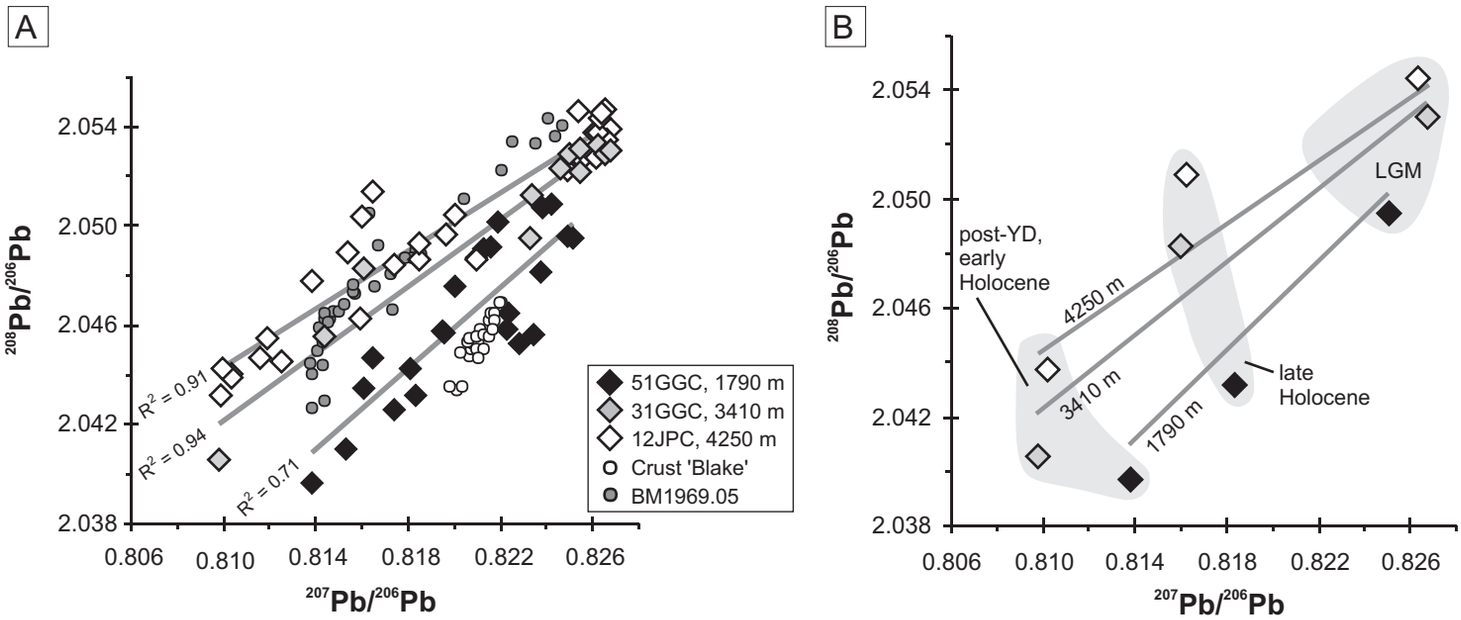

Figure 6 - Gutjahr et al.

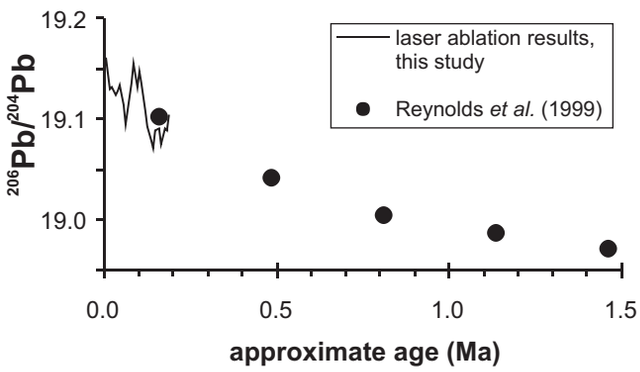

Figure 7 - Gutjahr et al.

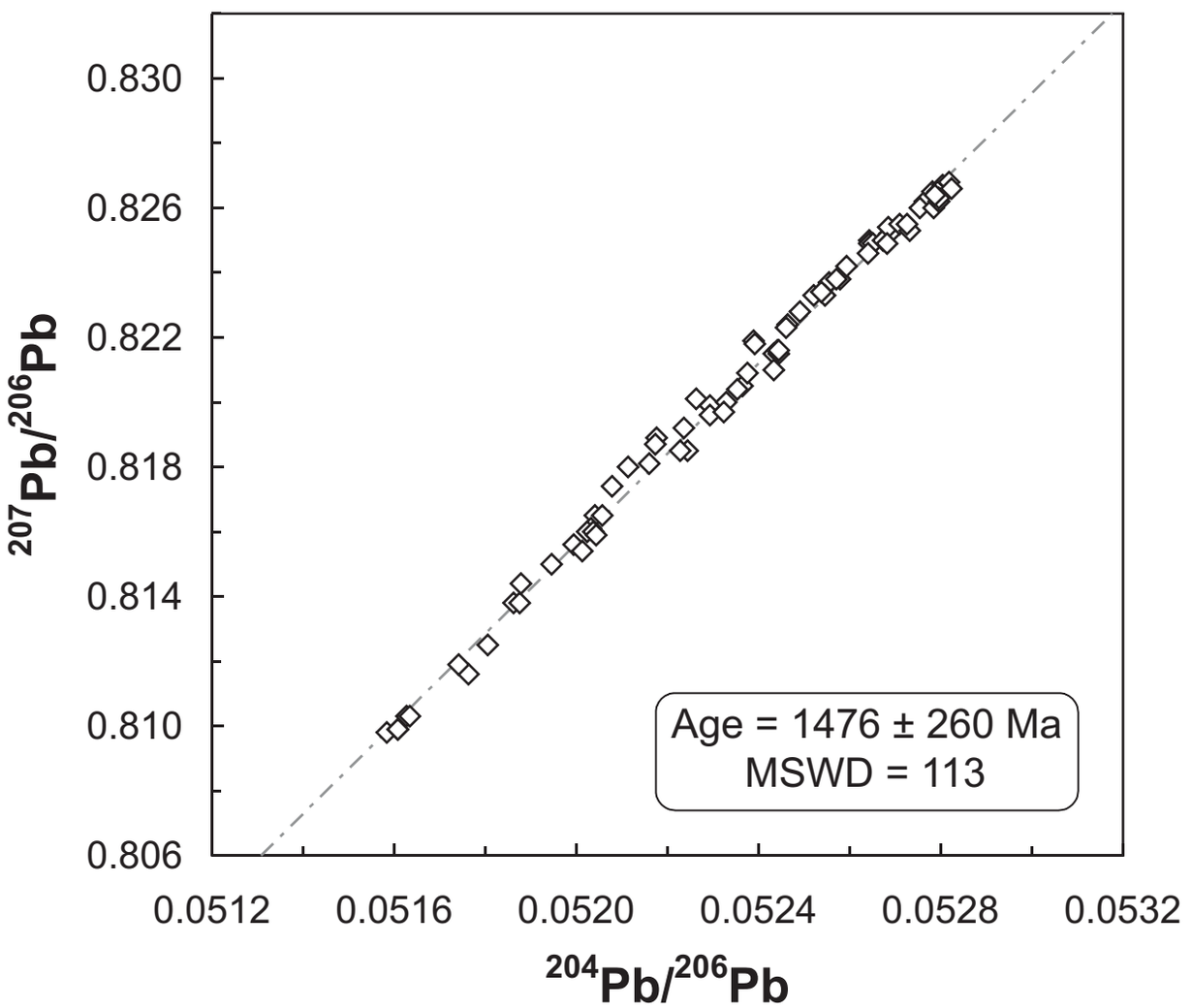

Figure 8 - Gutjahr et al.

Table 1. Lead isotope compositions of all analysed authigenic Fe-Mn oxyhydroxide samples

Depth in core (cm)	Calendar Age (ka BP)	$^{206}Pb/^{204}Pb$	$^{207}Pb/^{204}Pb$	$^{208}Pb/^{204}Pb$	$^{207}Pb/^{206}Pb$	$^{208}Pb/^{206}Pb$
Core 51GGC, 1790 m						
40 cm	1.59	19.088	15.690	39.133	0.8219	2.0502
duplicate		19.087	15.686	39.130	0.8218	2.0501
60 cm	2.39	19.166	15.695	39.191	0.8189	2.0448
duplicate		19.134	15.691	39.162	0.8201	2.0468
160 cm	6.36	19.189	15.697	39.194	0.8180	2.0425
duplicate		19.167	15.691	39.175	0.8187	2.0439
220 cm	8.75	19.202	15.696	39.223	0.8174	2.0426
260 cm	10.34	19.216	15.689	39.289	0.8165	2.0447
270 cm	10.73	19.219	15.684	39.274	0.8161	2.0435
290 cm	11.2	19.282	15.692	39.329	0.8138	2.0397
300 cm	12.06	19.251	15.689	39.283	0.8150	2.0405
duplicate		19.233	15.686	39.266	0.8156	2.0415
310 cm	12.89	19.172	15.684	39.192	0.8181	2.0443
316 cm	13.01	19.144	15.683	39.150	0.8192	2.0451
duplicate		19.123	15.678	39.131	0.8199	2.0463
330 cm	13.72	19.123	15.674	39.150	0.8196	2.0472
duplicate		19.097	15.669	39.106	0.8205	2.0478
350 cm	15.05	19.101	15.671	39.130	0.8204	2.0486
duplicate		19.072	15.667	39.076	0.8215	2.0488
370 cm	17.16	19.093	15.675	39.122	0.8209	2.0490
duplicate		19.068	15.665	39.074	0.8215	2.0492
371 cm	17.22	19.069	15.667	39.074	0.8216	2.0492
duplicate		19.068	15.666	39.074	0.8216	2.0492
373 cm	17.35	19.061	15.675	39.008	0.8224	2.0465
378 cm	17.65	19.062	15.674	38.996	0.8223	2.0458
385 cm	21.36	19.051	15.676	38.965	0.8228	2.0453
390 cm	22.15	19.040	15.675	38.942	0.8233	2.0453
duplicate		19.028	15.673	38.930	0.8237	2.0459
395 cm	22.94	19.019	15.669	39.004	0.8238	2.0507
400 cm	23.73	18.996	15.671	38.932	0.8250	2.0496
duplicate		18.980	15.662	38.898	0.8252	2.0494
405 cm	24.52	18.996	15.669	38.933	0.8249	2.0495
duplicate		18.993	15.666	38.929	0.8249	2.0497
412 cm	25.62	19.022	15.669	38.958	0.8238	2.0481
422 cm	27.2	19.014	15.672	38.996	0.8242	2.0509

Table 1. continued. Samples analysed at the Bristol Isotope Group are denoted [a]

Depth in core (cm)	Appr. Calendar Age (ka BP)	$^{206}Pb/^{204}Pb$	$^{207}Pb/^{204}Pb$	$^{208}Pb/^{204}Pb$	$^{207}Pb/^{206}Pb$	$^{208}Pb/^{206}Pb$	
Core 31GGC, 3410 m							
20 cm		19.222	15.686	39.373	0.8160	2.0483	
30 cm		19.276	15.698	39.432	0.8144	2.0456	
72 cm		19.386	15.699	39.558	0.8098	2.0406	
135 cm		19.031	15.668	39.005	0.8233	2.0495	
140 cm		18.997	15.664	38.987	0.8246	2.0523	
150 cm		18.985	15.663	38.973	0.8250	2.0529	
260 cm		18.981	15.667	38.970	0.8254	2.0531	
275 cm		19.034	15.672	39.043	0.8234	2.0512	
330 cm		18.972	15.661	38.934	0.8255	2.0522	
390 cm		18.952	15.658	38.913	0.8262	2.0533	
410 cm		18.946	15.659	38.894	0.8265	2.0529	
420 cm		18.938	15.657	38.882	0.8267	2.0530	
Core 12JCP, 4250 m							
20 cm	3.2	19.210	15.684	39.406	0.8165	2.0514	
duplicate		19.217	15.681	39.402	0.8160	2.0504	
30 cm	4.81	19.226	15.677	39.394	0.8154	2.0489	
40 cm	6.41	19.277	15.689	39.476	0.8138	2.0478	[a]
50 cm	8.01	19.319	15.680	39.502	0.8116	2.0447	
duplicate		19.327	15.692	39.535	0.8119	2.0455	[a]
55 cm	8.81	19.370	15.696	39.594	0.8103	2.0441	
duplicate		19.377	15.693	39.591	0.8099	2.0432	
duplicate		19.367	15.694	39.585	0.8103	2.0439	[a]
63 cm	10.09	19.377	15.694	39.612	0.8099	2.0443	[a]
69 cm	11	19.303	15.684	39.467	0.8125	2.0446	
74 cm	11.71	19.215	15.678	39.318	0.8159	2.0463	[a]
77 cm	12.14	19.141	15.667	39.216	0.8185	2.0487	
duplicate		19.147	15.671	39.237	0.8185	2.0493	[a]
85 cm	12.67	19.110	15.670	39.184	0.8200	2.0504	
duplicate		19.112	15.665	39.173	0.8197	2.0497	
102 cm	13.38	19.072	15.658	39.073	0.8210	2.0487	
117 cm	14	18.964	15.652	38.966	0.8253	2.0547	
140 cm	14.95	18.982	15.659	38.957	0.8249	2.0522	
156 cm	15.62	18.966	15.657	38.931	0.8255	2.0527	
172 cm	16.28	18.942	15.656	38.921	0.8265	2.0547	
193 cm	17.15	18.956	15.659	38.932	0.8260	2.0538	
203 cm	17.57	18.945	15.647	38.891	0.8260	2.0529	
220 cm	18.27	18.941	15.648	38.879	0.8262	2.0527	
233 cm	18.73	18.933	15.653	38.886	0.8268	2.0539	
duplicate		18.931	15.649	38.874	0.8266	2.0535	
251 cm	19.56	18.941	15.650	38.902	0.8262	2.0538	
263 cm	20.05	18.941	15.652	38.913	0.8263	2.0543	
duplicate		18.944	15.654	38.921	0.8264	2.0545	

Table S1. Laser ablation Pb isotope results of crust 'Blake'

Distance (µm)	Age (ka)	+	-	208Pb int [V]	$^{206}Pb/^{204}Pb$	2σ	$^{207}Pb/^{204}Pb$	2σ	$^{208}Pb/^{204}Pb$	2σ	$^{207}Pb/^{206}Pb$	2σ	$^{208}Pb/^{206}Pb$	2σ
15	8	10	10	1.02	19.160	0.009	15.715	0.008	39.148	0.020	0.82013	0.00012	2.0434	0.00029
30	16	10	10	0.99	19.129	0.009	15.699	0.006	39.122	0.015	0.82062	0.00014	2.0448	0.00039
45	24	10	10	1.04	19.132	0.007	15.701	0.007	39.121	0.017	0.82075	0.00011	2.0451	0.00027
60	32	10	10	0.97	19.125	0.009	15.699	0.008	39.113	0.021	0.82082	0.00010	2.0453	0.00029
75	40	10	10	0.87	19.128	0.011	15.707	0.009	39.137	0.024	0.82110	0.00008	2.0458	0.00025
90	48	10	10	0.92	19.134	0.010	15.720	0.008	39.152	0.020	0.82149	0.00010	2.0462	0.00029
105	56	10	10	0.97	19.114	0.008	15.704	0.007	39.118	0.018	0.82160	0.00008	2.0465	0.00022
120	63	10	10	0.87	19.095	0.011	15.690	0.009	39.079	0.023	0.82176	0.00011	2.0465	0.00029
135	71	10	10	0.70	19.123	0.012	15.703	0.010	39.117	0.025	0.82105	0.00011	2.0453	0.00030
150	79	10	10	0.78	19.136	0.012	15.697	0.010	39.105	0.027	0.82034	0.00011	2.0436	0.00030
165	87	10	10	0.74	19.155	0.011	15.702	0.010	39.147	0.026	0.81975	0.00013	2.0436	0.00021
180	95	10	10	0.86	19.131	0.012	15.693	0.010	39.123	0.026	0.82026	0.00011	2.0449	0.00021
195	103	10	10	1.02	19.148	0.009	15.709	0.008	39.158	0.020	0.82054	0.00011	2.0453	0.00029
210	111	10	10	0.93	19.135	0.010	15.702	0.008	39.133	0.021	0.82063	0.00014	2.0455	0.00028
225	119	10	10	0.78	19.108	0.009	15.688	0.007	39.082	0.020	0.82098	0.00014	2.0455	0.00028
240	127	10	10	0.98	19.094	0.010	15.675	0.009	39.044	0.021	0.82097	0.00010	2.0450	0.00025
255	135	10	10	0.88	19.080	0.012	15.671	0.010	39.032	0.027	0.82125	0.00009	2.0456	0.00024
270	143	10	10	0.79	19.071	0.013	15.667	0.011	39.010	0.028	0.82147	0.00010	2.0456	0.00019
285	151	10	10	0.78	19.089	0.010	15.684	0.008	39.055	0.020	0.82171	0.00009	2.0462	0.00023
300	159	10	10	0.80	19.091	0.012	15.696	0.011	39.081	0.027	0.82205	0.00010	2.0469	0.00024
315	167	10	10	1.01	19.074	0.009	15.677	0.008	39.036	0.019	0.82199	0.00007	2.0469	0.00021
330	175	10	10	1.16	19.090	0.007	15.687	0.006	39.052	0.015	0.82167	0.00010	2.0459	0.00026
345	182	10	10	1.10	19.089	0.008	15.677	0.007	39.039	0.018	0.82129	0.00010	2.0451	0.00029
360	190	10	10	1.03	19.104	0.008	15.685	0.007	39.061	0.018	0.82104	0.00010	2.0447	0.00027